Dalton Transactions

PAPER

Cite this: *Dalton Trans.*, 2015, **44**, 3342

Chemical, radiochemical and biological studies of new gallium(III) complexes with hexadentate chelators†

Francisco Silva,[a] Maria Paula C. Campello,[a] Lurdes Gano,[a] Célia Fernandes,[a] Isabel C. Santos,[a] Isabel Santos,[a] José R. Ascenso,[b] M. João Ferreira[b] and António Paulo*[a]

Received 25th July 2014,
Accepted 17th December 2014

DOI: 10.1039/c4dt02274b

www.rsc.org/dalton

New N_4O_2-donor acyclic chelators 2-[[2-[2-(3,5-dimethylpyrazol-1-yl)ethyl-[2-[(2-hydroxyphenyl)-methylamino]ethyl]amino]ethylamino]methyl]phenol ($H_2L^{pz*,NH}$) and 2-[[2-[2-[(2-hydroxyphenyl)methyl-amino]ethyl-(2-pyridylmethyl)amino]ethylamino]methyl]phenol ($H_2L^{py,NH}$) were obtained upon introduction of pyridyl or pyrazolyl coordinating units at the central nitrogen atom of diethylenetriamine (dien) and by functionalization of its terminal amines with phenol groups. The coordination behavior of $H_2L^{pz*,NH}$ and $H_2L^{py,NH}$ was evaluated towards $^{nat}Ga/^{67}Ga$, aiming to assess their suitability to obtain Ga(III) chelates relevant for biomedical applications. Single crystal X-ray diffraction analysis of the complexes $[GaL^{pz*,NH}](ClO_4)$ and $[GaL^{py,NH}](ClO_4)$ confirmed the presence of N_4O_2-hexadentate chelators with the phenoxide groups coordinated *cis* relatively to the pyridyl/pyrazolyl arms. Unlike $[GaL^{pz*,NH}](ClO_4)$, $[GaL^{py,NH}](ClO_4)$ exists in solution as a mixture of isomers, as confirmed by several NMR techniques. The corresponding radiocomplex $[^{67}GaL^{py,NH}]^+$ was obtained smoothly in almost quantitative radiochemical yield, contrary to $[^{67}GaL^{pz*,NH}]^+$ that seems to be (hemi)labile under the same conditions. $[^{67}GaL^{py,NH}]^+$ presents a high *in vivo* stability and a favourable biodistribution profile in mice. The imine congeners 2-[(*E*)-2-[2-(3,5-dimethylpyrazol-1-yl)ethyl-[2-[(*E*)-(2-hydroxyphenyl)methyleneamino]ethyl]amino]ethyliminomethyl]phenol ($H_2L^{pz*,C=N}$) and 2-[(*E*)-2-[2-[(*E*)-(2-hydroxyphenyl)methyleneamino]ethyl-(2-pyridylmethyl)amino]ethyl-iminomethyl]phenol ($H_2L^{py,C=N}$) were also evaluated but they did not form complexes compatible for biomedical applications owing to their high reactivity.

Introduction

Metal-based compounds have an increasing importance in most prominent biomedical applications, as they offer the possibility of exploring a higher variety of structural motifs and reactivity patterns when compared with purely organic molecules. Together with the design of cytotoxic anti-cancer drugs, the development of radiopharmaceuticals can be considered as the most important application of coordination and organometallic complexes of transition and post-transition metals. Radiopharmaceuticals are drugs containing a radionuclide in their composition and are used in nuclear medicine for diagnosis and therapy. For diagnosis, there are two modalities, single photon emission computed tomography (SPECT) and positron emission tomography (PET), which make use of gamma- or positron-emitting radionuclides, respectively.

Gallium complexes have emerged as one of the most promising new classes of cytotoxic drugs and diagnostic radiopharmaceuticals.[1–6] In particular, gallium-67 and gallium-68 complexes are suitable for SPECT and PET imaging, respectively. Moreover, ^{68}Ga is available from the $^{68}Ge/^{68}Ga$ generator, which allows the possibility of obtaining a PET radionuclide without requiring the presence of a nearby cyclotron.[7] This possibility anticipates a bright future for ^{68}Ga in PET imaging, in the same way as ^{99m}Tc became the workhorse of SPECT imaging several years ago.

[a]*Centro de Ciências e Tecnologias e Nucleares, IST, Universidade de Lisboa, Estrada Nacional 10, 2695-066 Bobadela LRS, Portugal. E-mail: apaulo@ctn.ist.utl.pt*
[b]*Centro de Quimica Estrutural, IST, Universidade de Lisboa, Avenida Rovisco Pais 1, 1049-001 Lisboa, Portugal*

†Electronic supplementary information (ESI) available: Crystallographic information files (CIF) for X-ray structures of compounds $[GaL^{pz*,OMe}](ClO_4)$, $[GaL^{pz*,NH}](ClO_4)$ and $[GaL^{py,NH}](ClO_4)$. Details on the synthesis and characterization of $[GaL^{pz*,OMe}](ClO_4)$. ^1H and ^{71}Ga NMR spectra and two dimensional $^1H–^1H$ COSY and $^1H–^{13}C$ HSQC spectra for all complexes. $^1H–^{15}N$ HSQC, NOESY and TOCSY spectra for $[GaL^{py,NH}](ClO_4)$. Tables with biodistribution data in mice for $[^{67}GaL^{py,NH}]^+$. HPLC chromatograms of $[^{67}GaL^{py,NH}]^+$ in the presence of human *apo*-transferrin. HPLC chromatograms of urine and serum from mice injected with $[^{67}GaL^{py,NH}]^+$. CCDC 964822–964825. For ESI and crystallographic data in CIF or other electronic format see DOI: 10.1039/c4dt02274b

Like for other radiometals, the biodistribution of ^{67}Ga/^{68}Ga complexes to be evaluated as radiopharmaceuticals depends on their chemical and physical properties – perfusion radiopharmaceuticals – or on their biological interactions – target-specific radiopharmaceuticals. The biological distribution of *perfusion agents* is determined by blood flow and these agents target high capacity systems, such as phagocytosis, hepatocyte clearance and glomerular filtration. The target-specific radiopharmaceuticals target low capacity systems, and their biodistribution is determined by specific protein interactions, for example antigen and enzymatic or receptor-binding interactions.[8] Inorganic chemists play an important role in the design of perfusion or target-specific $^{67/68}$Ga radiopharmaceuticals, as it is necessary to design and have available biocompatible chelators that form thermodynamically stable and kinetically inert Ga complexes. Ga(III) is a rather hard Lewis acid and, for this reason, macrocyclic or acyclic polyaminocarboxylic ligands (Chart 1) are among the most explored chelators to obtain stable and inert Ga complexes suitable for the design of radiopharmaceuticals.[5,6]

Macrocyclic ligands, like 1,4,7-triazacyclononane-1,4,7-triacetic acid (NOTA) and 1,4,7,10-tetraazacyclododecane-1,4,7,10-tetraacetic acid (DOTA), can afford Ga complexes of high kinetic inertness and thermodynamic stability that show a high resistance to *in vivo* transchelation processes.[6] These favorable features justify that bifunctional versions of NOTA and DOTA have been thoroughly applied in the ^{67}Ga- or ^{68}Ga-labeling of clinically relevant biomolecules, namely in the case of biologically active peptides.[3,5] Very good results were obtained for ^{68}Ga-DOTATOC and ^{68}Ga-DOTANOC, which are radiometallated analogues of somatostatin (SST) clinically used to image SST-receptor positive malignancies.[9] However, the synthesis of suitable macrocyclic bifunctional chelators for the conjugation of the biomolecules and still capable of stabilizing the metal ion can be considerably challenging, as only one of the pendant arms must be selectively functionalized with the targeting molecule. For this reason, several research groups have pursued in recent years the synthesis and evaluation of acyclic chelators suitable for the stable complexation of ^{67}Ga and ^{68}Ga under physiological conditions. Recently, encouraging results have been reported for linear and potentially hexadentate ligands (*e.g.* HBED, H_2dedpa and CP256 (Chart 1)), which have been successfully applied in ^{67}Ga/^{68}Ga-labelling of peptides and proteins.[10–13] Moreover, acyclic chelators might also be useful for the design of gallium-based perfusion radiopharmaceuticals.[14–17] For instance, several N_4O_2-donor Schiff bases of the bis(salicyladimine) type, namely BAPDMEN derivatives (Chart 1), have been applied to obtain cationic and lipophilic ^{67}Ga/^{68}Ga complexes for cardiac perfusion imaging or for *in vivo* detection of multidrug resistance.[15–17]

In the past few years, our group has been involved in the study of Ga(III) complexes of biomedical relevance, either as cytotoxic drugs or as radiopharmaceuticals.[18,19] Within our interest on gallium-based (radio)pharmaceuticals, we have embarked on the synthesis of new N_4O_2-donor acyclic ligands and we have evaluated their coordination capability towards the Ga(III) metal ion, aiming to have an insight on their potential usefulness as hexadentate chelators for radiopharmaceutical research. These N_4O_2-donor ligands (2-[[2-[2-(3,5-

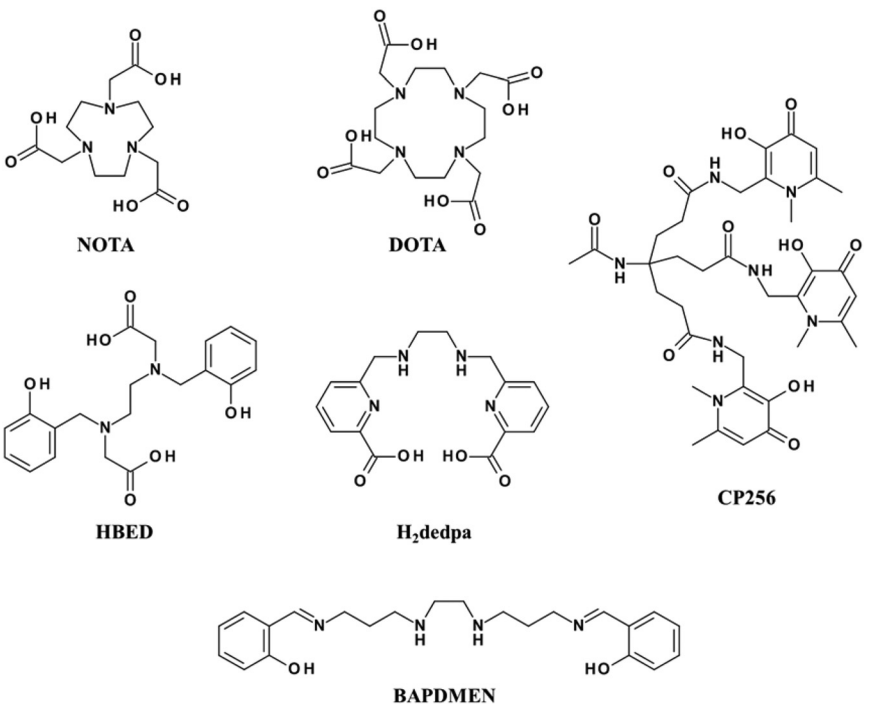

Chart 1 Selected examples of acyclic and cyclic chelators used in the design of perfusion or target-specific gallium radiopharmaceuticals.

dimethylpyrazol-1-yl)ethyl-[2-[(2-hydroxyphenyl)methylamino]-ethyl]amino]ethylamino]methyl]phenol ($\mathbf{H_2L^{pz*,NH}}$) and 2-[[2-[2-[(2-hydroxyphenyl)methylamino]ethyl-(2-pyridylmethyl)amino]-ethylamino]methyl]phenol ($\mathbf{H_2L^{py,NH}}$)), featuring a N-heterocyclic pendant arm of the pyridyl and pyrazolyl type and two phenolate coordinating groups, have been designed based on the diethylenetriamine (dien) framework and were obtained by reduction of the corresponding Schiff bases 2-[(*E*)-2-[2-(3,5-dimethylpyrazol-1-yl)ethyl-[2-[(*E*)-(2-hydroxyphenyl)methylene-amino]ethyl]amino]ethyliminomethyl]phenol ($\mathbf{H_2L^{pz*,C=N}}$) and 2-[(*E*)-2-[2-[(*E*)-(2-hydroxyphenyl)methyleneamino]ethyl-(2-pyridylmethyl)amino]ethyliminomethyl]phenol ($\mathbf{H_2L^{py,C=N}}$), respectively. The selected N-heterocyclic groups have a well documented capacity of coordinating different metal centers under the aqueous conditions required in radiopharmaceutical chemistry.[11,12,20–22] By proposing these ligands, we also took into consideration that they can be obtained in a modular way in a few steps, by combination of the desired N-heterocyclic and phenol derivatives. Therefore, these N_4O_2-donors are easily tunable upon introduction of different substituents (*e.g.* alkyl or ether groups) in the dien backbone and/or in the different aromatic rings, while offering the possibility of a selective functionalization of the N-heterocyclic rings with groups (*e.g.* –COOH) suitable for further coupling of bioactive molecules. We have anticipated that this versatile tunability would help in the modulation/optimization of the physico-chemical properties of the respective Ga(III) complexes as perfusion radiopharmaceuticals, *e.g.* for myocardial imaging, as well as in their use as potential bifunctional chelators for the design of target-specific radiopharmaceuticals.

In this manuscript, the synthesis of $\mathbf{H_2L^{pz*,NH}}$ and $\mathbf{H_2L^{py,NH}}$ and the evaluation of their coordination behavior towards the Ga^{3+} ion are reported. Herein, we also discuss the molecular structures of the resulting Ga(III) complexes, which were assessed in solution and in the solid state based on multinuclear NMR studies and X-ray diffraction analysis, respectively. In parallel, the coordination behavior of the precursor Schiff base ligands, $\mathbf{H_2L^{pz*,C=N}}$ and $\mathbf{H_2L^{py,C=N}}$, towards Ga^{3+} was also investigated. For those complexes that were obtained as well-identified species, the synthesis of the radioactive congeners was attempted using ^{67}Ga and their *in vitro* stability was tested under transchelation experiments with transferrin, and their biodistribution and pharmacokinetics were evaluated in mice.

Results and discussion

Synthesis of ligands and Ga(III) complexes

The synthesis of the N_4O_2-donor ligands was initiated with the introduction of the pyrazolyl- and pyridyl-containing pendant arms at the central nitrogen atom of the dien backbone (Scheme 1). This comprised the synthesis of the previously reported compound (2-{(2-*tert*-butoxycarbonylaminoethyl)-[2-(3,5-dimethylpyrazol-1-yl)-ethyl]amino}ethyl) carbamic acid *tert*-butyl ester (**2**), which was obtained by the literature method.[23] The pyridyl congener, *i.e. tert*-butyl *N*-[2-[2-(*tert*-butoxycarbonylamino)ethyl-(2-pyridylmethyl)amino]ethyl]carbamate (**4**), was obtained in a similar way by N-alkylation of *N*,*N*′-bis(*tert*-butoxycarbonyl)diethylenetriamine (**1**) with 1-bromomethylpyridine. Removal of the BOC protecting groups of **2** and **4**, under acid hydrolysis, afforded respectively compounds **3** and **5** containing two terminal primary amines. Treatment of **3** and **5** with salicylaldehyde in refluxing methanol, using a 1 : 2 molar ratio of the reagents, gave the Schiff-base ligands

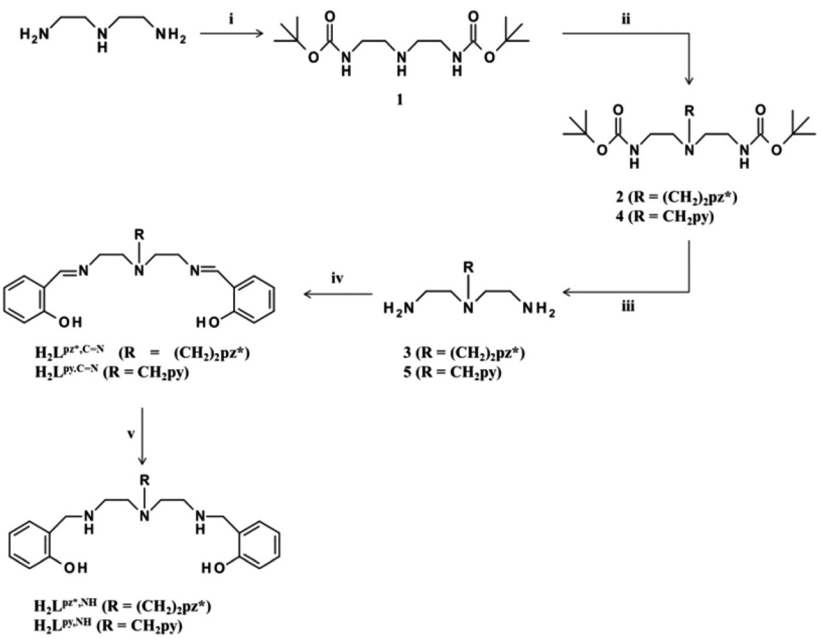

Scheme 1 Synthesis of the ligands. (i) $O(BOC)_2$, THF, r.t., o.n.; (ii) $BrCH_2CH_2$(3,5-Me_2pz) or 2-$BrCH_2$py, K_2CO_3, KI, THF, reflux, 24 h; (iii) HCl/MeOH, r.t., 2 h; (iv) salicylaldehyde, MeOH, reflux, 4 h; (v) $NaBH_4$, MeOH, r.t., o.n.

$H_2L^{pz*,C=N}$ and $H_2L^{py,C=N}$, respectively. The corresponding reduced derivatives, $H_2L^{pz*,NH}$ and $H_2L^{py,NH}$, were synthesized by the reaction of $H_2L^{pz*,C=N}$ and $H_2L^{py,C=N}$ with sodium borohydride in methanol. After appropriate work-up, these new N_4O_2-donor ligands were obtained as pale yellow oils in moderate to high yields. Their characterization was done by HR-ESI-MS, IR, ^1H and ^{13}C NMR spectroscopy, which confirmed the formulation proposed for the compounds. In particular, the ^1H NMR spectra of $H_2L^{pz*,C=N}$ and $H_2L^{py,C=N}$ in $CDCl_3$ showed a downfield singlet at 8.05 ppm due to the imine N=CH–Ar proton. These imine proton resonances are absent in the ^1H NMR spectra of $H_2L^{pz*,NH}$ and $H_2L^{py,NH}$ confirming the reduction of the imine function, which is further corroborated by the presence in the spectra of both compounds of a singlet at 3.89 ppm due to the protons of the new CH_2 group.

As shown in Scheme 2, the attempts to synthesize the Ga(III) complexes with $H_2L^{pz*,NH}$ and $H_2L^{py,NH}$ were made by the reaction with gallium nitrate in methanol in the presence of sodium acetate, followed by precipitation with $NaClO_4$. These reactions led to the formation of $[GaL^{pz*,NH}](ClO_4)$ and $[GaL^{py,NH}](ClO_4)$, which were isolated in the pure form in low to moderate yields. These yields are justified by the purification processes needed to separate any free ligand and/or free gallium. Their characterization comprised ESI-MS, C,H,N analysis, X-ray diffraction analysis, IR and 1D and 2D multinuclear NMR.

We have also investigated the capability of the imine derivatives to form gallium complexes suitable for *in vivo* studies but the complexes were highly susceptible to decomposition reactions originating from the well-known high reactivity of the imine linkage. From these studies, the only isolated complex was $[GaL^{pz*,OMe}](ClO_4)$ coordinated by a hexadentate hemiaminal derivative as a result of the attack of one of the imine groups of $L^{pz*,C=N}$ by methanol. See ESI† for full details and characterization of $[GaL^{pz*,OMe}](ClO_4)$.

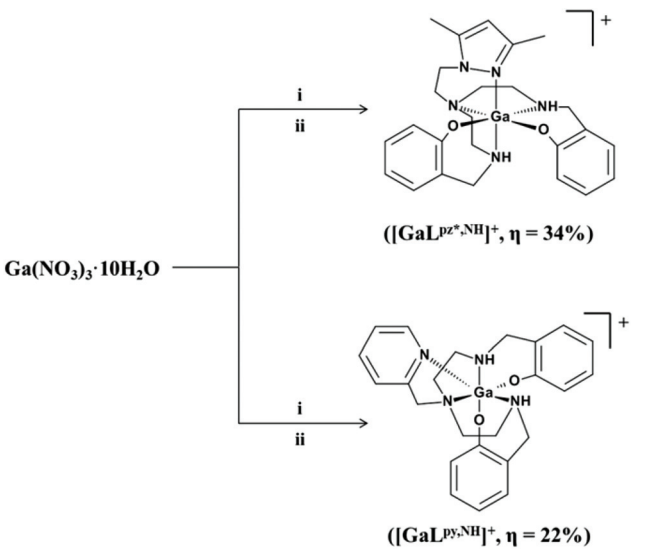

Scheme 2 Synthesis of the gallium complexes. (i) $H_2L^{pz*,NH}$ or $H_2L^{py,NH}$, $NaCH_3COO$, MeOH, r.t., o.n.; (ii) $NaClO_4$.

Solid state molecular structures

Crystals of $[GaL^{pz*,NH}](ClO_4)$ and $[GaL^{py,NH}](ClO_4)$ suitable for X-ray diffraction analysis were obtained from slow evaporation of concentrated solutions of the compounds in methanol. For $[GaL^{pz*,NH}](ClO_4)$, X-ray quality crystals were also grown from a concentrated solution of the compound in chloroform. A summary of the crystal data, structure solution and refinement parameters are given in Table 1. A selection of bond lengths and angles is presented in Table 2.

The molecular structures of the cations of $[GaL^{pz*,NH}](ClO_4)$ and $[GaL^{py,NH}](ClO_4)$ are shown in Fig. 1 and 2, respectively. Both compounds possess three chiral coordinated nitrogen atoms. For $[GaL^{pz*,NH}](ClO_4)$, the measured crystals contain a unique enantiomeric form in the asymmetric unit, having *S*, *R* and *R* absolute configurations at the N1, N2 and N3 nitrogen atoms, either when the crystals were obtained from concentrated methanol or chloroform solutions of the compound. In contrast, for $[GaL^{py,NH}](ClO_4)$ there are two independent molecules in the asymmetric unit corresponding to two enantiomers with *S*, *R*, *R* and *R*, *S*, *S* absolute configurations at the N1, N2 and N3 nitrogen atoms, respectively (Fig. 2).

The Ga–O, Ga–Npz and Ga–Npy bond distances of $[GaL^{pz*,NH}](ClO_4)$ and $[GaL^{py,NH}](ClO_4)$ span in the range 1.874(2)–1.9158(17) Å, 2.121(2)–2.144(3) Å and 2.0838(14)–2.0941(14) Å, respectively. These values compare well with those reported for other Ga(III) complexes containing phenoxide, pyrazolyl and pyridyl coordinating groups.[11,18,24,25] The Ga–N bond distances of the coordinated pyrazolyl ring in $[GaL^{pz*,NH}](ClO_4)$, Ga–N = 2.121(2) Å in crystals obtained from $CHCl_3$ and Ga–N = 2.144(3) Å in the crystals obtained from MeOH are slightly longer than the Ga–N bond distances found in the coordinated pyridyl rings in the two enantiomeric forms that are present in the measured crystal of $[GaL^{py,NH}](ClO_4)$ (Ga–N = 2.0941(14) Å in molecule A and Ga–N = 2.0838(14) Å in molecule B). This trend reflects most probably the poorer electron-releasing properties of pyrazolyl, together with the greatest rigidity inherent to the pyridyl-containing five-membered $[GaN_2C_2]$ chelating ring in comparison with the pyrazolyl-containing six-membered $[GaN_3C_2]$ chelating ring.

Solution NMR structural analysis

Octahedral complexes of the type MA_2B_2CD with hexadentate chelators based on the dien framework can exist as *fac* isomers, containing the three dien nitrogen atoms coordinated in the same face of the octahedron, or as *mer* isomers where the same nitrogen atoms occupy a meridional plane. $[GaL^{pz*,NH}]^+$ and $[GaL^{py,NH}]^+$ cations can therefore exist as *fac* and/or *mer* isomers in solution.

Compounds $[GaL^{pz*,NH}](ClO_4)$ and $[GaL^{py,NH}](ClO_4)$ were studied by a variety of multinuclear and bidimensional NMR techniques to identify the number of species in solution and assign the coordination mode of the respective chelators in solution. The assignment of the different diastereotopic

Table 1 Crystallographic details of the gallium complexes[a]

	$[GaL^{pz*,NH}](ClO_4)\cdot(MeOH)$	$[GaL^{pz*,NH}](ClO_4)\cdot(CHCl_3)$	$[GaL^{py,NH}](ClO_4)\cdot(MeOH)$
Empirical form.	$C_{26}H_{37}N_5O_7ClGa$	$C_{26}H_{34}N_5O_6Cl_4Ga$	$C_{24}H_{28}N_4O_6ClGa$
f_w	636.78	724.10	573.67
Temp. (K)	150(2)	150(2)	150(2)
Cryst. System	Monoclinic	Monoclinic	Monoclinic
Space group	$P2_1/c$	$P2_1/c$	$P2_1/n$
a (Å)	7.9018(3)	14.2384(5)	22.5793(5)
b (Å)	11.6269(4)	12.5399(4)	10.5056(2)
c (Å)	30.2610(11)	17. 0528(6)	23.2529(4)
α (°)	90	90	90
β (°)	91.358(1)	98.761(1)	117.545(1)
γ (°)	90	90	90
V (Å^3)	2779.40(17)	3009.22(18)	4890.57(18)
Z, D_{calcd} (Mg m^{-3})	4, 1.522	4, 1.598	8, 1.558
μ (mm^{-1})	1.141	1.319	1.283
F(000)	1328	1488	2368
θ range (°)	2.67–25.34	2.59–25.35	3.25–25.68
h,k,l range	−9/9,−13/14,−36/30	−16/17,−15/11,−20/20	−27/19,−12/12,−24/28
Reflns col./uniq.	13 307/5077 [R_{int} = 0.0440]	21 810/5497 [R_{int} = 0.0552]	72 909/9277 [R_{int} = 0.0444]
T max./min.	0.8945/0.7714	0.9018/0.7601	0.8210/0.6551
S on F^2	1.072	1.070	1.046
R_1 ($I > 2\sigma(I)$)	0.0395	0.0432	0.0252
wR_2 (all data)	0.0942	0.1027	0.0609

[a] Definitions: $R_1 = \sum||F_o| - |F_c||/\sum|F_o|$, $wR_2 = [\sum w(F_o^2 - F_c^2)^2/\sum w(F_o^2)^2]^{1/2}$.

Table 2 Selected bond lengths (Å) and angles (°) of the gallium complexes

			$[GaL^{py,NH}](ClO_4)\cdot(MeOH)$	
	$[GaL^{pz*,NH}](ClO_4)\cdot(MeOH)$	$[GaL^{pz*,NH}](ClO_4)\cdot(CHCl_3)$	**mol A**	**mol B**
Ga1–O1	1.9158(17)	1.886(2)	1.9021(12)	1.9003(12)
Ga1–O2	1.8879(19)	1.874(2)	1.8800(12)	1.8753(12)
Ga1–N1	2.127(2)	2.121(3)	2.0900(15)	2.0870(15)
Ga1–N2	2.165(2)	2.157(3)	2.1329(15)	2.1389(15)
Ga1–N3	2.073(2)	2.116(3)	2.1203(15)	2.1220(14)
Ga1–N4	2.121(2)	2.144(3)	2.0941(14)	2.0838(14)
O1–Ga1–O2	94.12(8)	97.64(10)	95.91(5)	95.40(5)
O1–Ga1–N1	90.71(8)	91.87(10)	90.74(5)	90.11(6)
O2–Ga1–N1	90.77(9)	90.42(10)	97.63(6)	99.21(6)
O1–Ga1–N4	84.72(8)	84.77(10)	85.13(5)	86.17(5)
O2–Ga1–N4	96.05(8)	97.15(9)	99.89(6)	98.72(6)
N1–Ga1–N4	72.04(9)	172.05(10)	162.32(6)	161.95(6)
O1–Ga1–N3	172.77(9)	171.32(10)	172.65(6)	172.58(6)
O2–Ga1–N3	92.24(9)	90.70(10)	90.42(5)	91.32(5)
N1–Ga1–N3	92.63(9)	90.46(10)	92.12(6)	91.93(6)
N4–Ga1–N3	91.21(9)	91.84(10)	90.12(6)	89.70(6)
O1–Ga1–N2	93.64(8)	91.61(10)	92.15(5)	91.15(5)
O2–Ga1–N2	169.14(8)	168.20(10)	171.92(5)	173.25(5)
N1–Ga1–N2	81.54(9)	81.93(10)	82.85(6)	82.40(6)
N4–Ga1–N2	92.22(9)	90.95(9)	80.14(6)	80.03(6)
N3–Ga1–N2	80.53(9)	80.44(10)	81.50(6)	82.06(6)

methylenic protons of all species and the corresponding carbon atoms was achieved by means of COSY and HSQC spectra, and in the case of $[GaL^{py,NH}]^+$ also by TOCSY experiments (see ESI†).

The ^{1}H and ^{13}C spectra of $[GaL^{pz*,NH}]^+$ in acetonitrile solution revealed the presence of a major species in solution, as can be checked in the ^{1}H NMR spectrum that is shown in Fig. S3.† The NOESY spectrum of such species (Fig. 3) shows negative NOE cross peaks between each pair of diastereotopic protons, which denotes slow exchange between enantiomers. This process also gives rise to indirect NOE effects. To aid in the assignment of the coordination geometry of the complex a series of selective NOE 1D spectra were also run (Fig. S9†). Based on these data, we concluded that the pyrazolyl ring occupies an axial position of the octahedron, while the opposite axial position is occupied by the NH group at 3.59 ppm (Fig. 3). In agreement with this coordination mode, the protons from the pyrazolyl methyl substituent appearing at 2.35 ppm are NOE-correlated with a CH_2 proton at 3.97 ppm from one of the six-membered rings containing a phenoxide

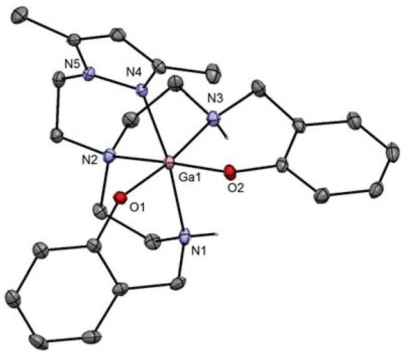

Fig. 1 ORTEP drawing at the 40% probability level for the $[GaL^{pz*,NH}]^+$ cation in $[GaL^{pz*,NH}]ClO_4$. Hydrogen atoms are omitted for clarity with the exception of those attached to the coordinating aliphatic amine groups.

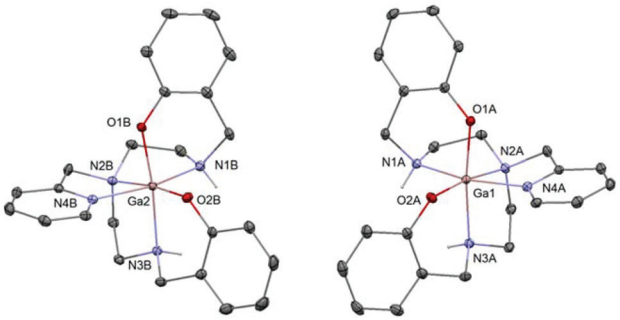

Fig. 2 ORTEP drawing at the 40% probability level for the two enantiomers of the $[GaL^{py,NH}]^+$ cation in $[GaL^{py,NH}]ClO_4$. Hydrogen atoms are omitted for clarity with the exception of those attached to the coordinating aliphatic amine groups.

group. The NH proton at 3.65 ppm points downward and is only correlated with a CH_2 proton at 2.63 ppm from one of the five-membered chelating rings containing axially and equatorially coordinated aliphatic amine groups. Furthermore, the CH_2 proton of the pyrazolyl arm at 4.22 ppm is closer to an axial proton at 2.73 ppm from the same five-membered chelating ring. In contrast, its geminal counterpart at 4.45 ppm has no NOE correlations with any of the CH_2 protons of the other five-membered chelating rings. In conclusion, the results of NOESY experiments indicated that the structure of $[GaL^{pz*,NH}]^+$ in solution corresponds to the molecular structure that was determined in the solid state (Fig. 1). The minor species may correspond to a *mer*-N_3dien isomer but it was not identified because the amount in solution is too small to perform NMR studies.

Unlike $[GaL^{pz*,NH}](ClO_4)$, the dissolution of $[GaL^{py,NH}](ClO_4)$ in acetonitrile gives rise to three species detectable by NMR: two major species (**A** and **B**) and a minor species (**C**)

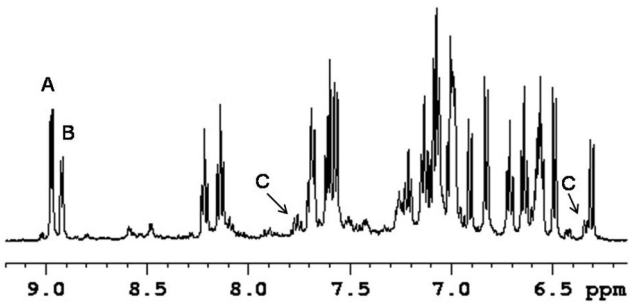

Fig. 4 Aromatic region of the ^1H spectrum of $[GaL^{py,NH}]^+$ in CD_3CN showing the presence of two major isomers **A** and **B** in a 1 : 0.6 ratio. Some of the peaks of the minor species **C** are also identified.

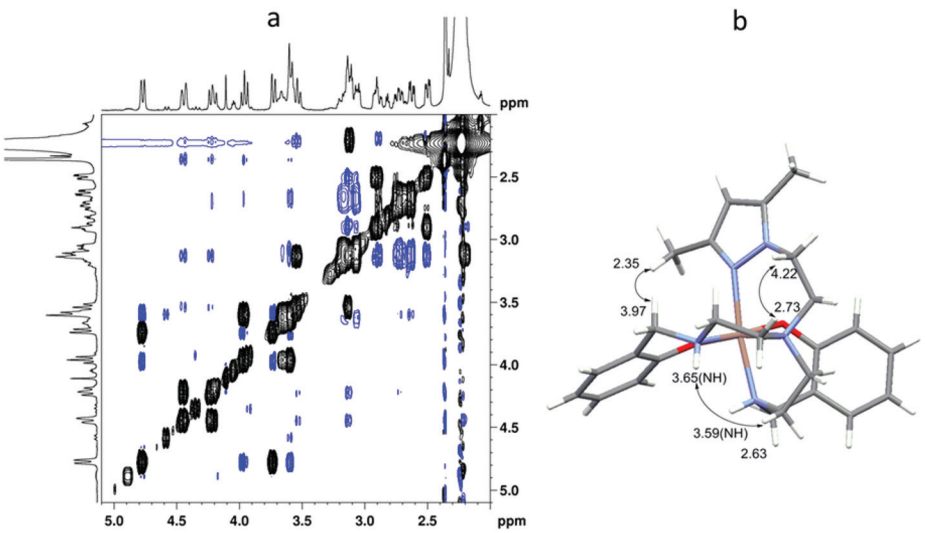

Fig. 3 (a) Aliphatic region of the NOESY spectrum of $[GaL^{pz*,NH}]^+$ in CD_3CN. A slow exchange process between enantiomers is manifested by the presence of negative NOE cross peaks between each pair of diastereotopic protons (black peaks). This process also gives rise to indirect NOE effects that are present in this spectrum. (b) Relevant NOE enhancements used to confirm the *fac*-N_3dien coordination of $GaL^{pz*,NH}$ in CD_3CN.

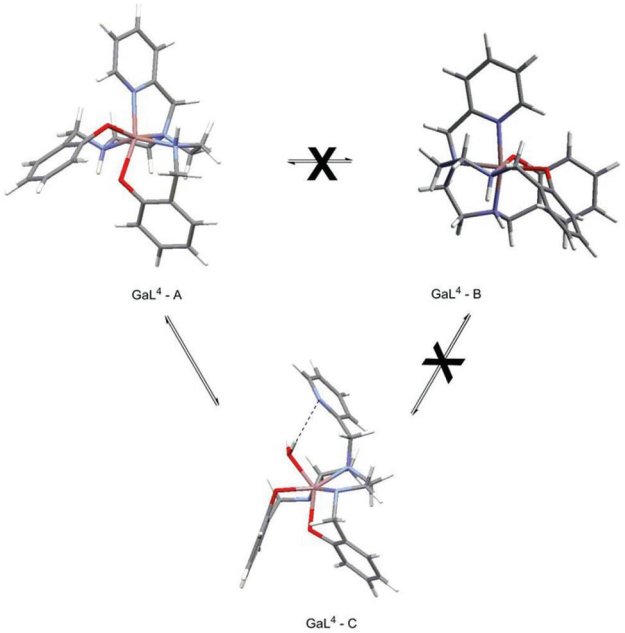

Scheme 3 $[GaL^{py,NH}]^+$ species present in acetonitrile solution.

(Fig. 4 and Scheme 3). **A** and **B** are coordination isomers and **C** is in exchange with **A**. This exchange process is most probably due to the replacement of the pyridyl arm by adventitious water.

The chemical shifts of the coordinated NH groups (Fig. 5 and Fig. S13†) are in general very similar for the three species indicating closely related structures in solution. The assignment of the diastereotopic methylenic protons in species **A** and **B** was achieved by combining the results of several NMR experiments such as COSY (Fig. S10†), TOCSY (Fig. S11†) and HSQC (Fig. S12†). For all species, the coordination geometry around the gallium ion is octahedral, as suggested by the careful analysis of the proton–proton correlations observed in the NOESY spectra (Fig. S14†).

In species **A** the pyridyl arm is *trans* to a phenolate oxygen and together with the three amine nitrogen donor atoms define two adjacent faces of an octahedron (Scheme 3). This corresponds to *mer*-N_3dien configuration because one phenolate oxygen is *cis* to the pyridyl arm and the other one is *trans*. The two five-membered chelating rings containing the aliphatic amines are puckered in a similar way but one of the NH protons (NH_a) lies on the same side as the pyridyl group while the other is pointing downward in the opposite direction (NH_b) (Fig. 5). Thus, NH_a at 4.16 ppm has a long range NOE with the CH_2 protons of the pyridyl arm resonating at 4.39 ppm while NH_b at 4.27 ppm does not correlate with these protons. The NH_a amine proton has also a very weak cross peak with the pyridyl H_o doublet at 8.97 ppm. This *ortho* proton shows another correlation with a CH_2 proton at 3.36 ppm from the phenoxide-containing six-membered ring in the opposite side of the molecule.

The isomer **B** also possesses an octahedral geometry but the pyridyl is now *trans* to the NH_a group (Fig. 5). The other two amine nitrogen atoms and NH_a belong to the same face of the octahedron. The NH_b proton at 3.79 ppm points downwards relative to the pyridyl arm and is directed towards NH_a at 4.16 ppm. Thus, NH_b has a long range NOE with NH_a; an axial CH_2 proton at 3.80 ppm from one of the phenoxide-containing six-membered chelating ring which correlates with the *ortho* proton from the pyridyl ring at 8.92 ppm (Fig. 5 and S14†). All these findings are consistent with the solid state molecular structures depicted in Fig. 2. We call this isomer *fac*-N_3dien because both phenoxide oxygens are *cis* to the pyridyl ring.

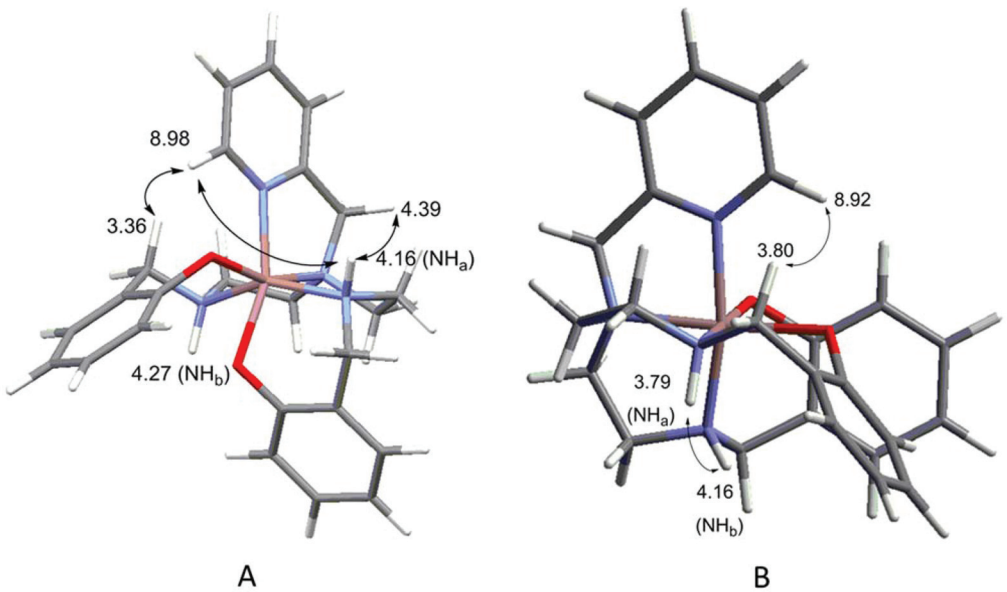

Fig. 5 Relevant NOE enhancements used to confirm the *mer*-N_3dien coordination in isomer **A** and the *fac*-N_3dien coordination in isomer **B** of $[GaL^{py,NH}]^+$ in CD_3CN.

The NOESY spectrum of $[GaL^{py,NH}]^+$ (Fig. S14†) in CD_3CN also shows negative cross peaks as a result of a slow exchange process that interconverts species **A** and **C** (black peaks). A variable temperature study (Fig. S15†) also confirmed the presence of this process. The *ortho* proton of the pyridyl ring in species **C** resonates at 8.22 ppm being considerably upfield shifted when compared with the same proton (δ = 8.92 ppm) in species **A**, and approaching the chemical shift of the *ortho* pyridyl proton in free $H_2L^{py,NH}$ (δ = 8.45 ppm). These data are consistent with the dissociation of the pyridyl group in **A**, which must be accompanied by the coordination of a solvent molecule. Rapid exchange in solution hampered its identification by NMR but we believe that adventitious water is probably replacing the pyridine arm instead of acetonitrile itself (Scheme 3). H_2O is a harder donor ligand than CH_3CN and, therefore, is expected to be a better ligand towards the oxophilic Ga^{3+} ion. Indeed, the ^{1}H NMR spectrum of $[GaL^{py,NH}]^+$ in D_2O shows that **B** and **C** are the predominant species in aqueous solutions (Fig. 6). The NOESY spectrum of $[GaL^{py,NH}]^+$ (Fig. S17†) in D_2O also shows negative cross peaks as a result of a slow exchange process that interconverts species **C** and **A** (black peaks). The variable temperature study (Fig. S18†) also confirms the presence of this process. The assignment of the diastereotopic CH_2 protons (Fig. S16†), based on a variety of 2D experiments (Fig. S19–S21†) associated with a fine analysis of the NOESY, confirmed that the structure of **B** is maintained in D_2O solution. Due to deuteration of NH protons and the scarce number of NOE contacts observed for **C**, it was impossible to confirm that the ligand arrangement in **C** matches that in **A**. However, the downfield shift of some CH_2 protons in **C** (Fig. S16†) is also observed in **A**, which seems to indicate that the ligand arrangement in these interconverting species is similar. The exception is the presence of a free pyridyl group in **C**, as indicated by *ortho* protons resonating at 8.19 ppm and without any long range NOE contacts (Fig. S17b†).

Despite the presence of two coordination isomers in solution, the ^{71}Ga NMR spectrum of $[GaL^{py,NH}]^+$ in acetonitrile displays a single but relatively broad resonance ($\Delta\nu_{1/2} \sim 5700$ Hz) centred at 102 ppm, which can be certainly accounted by the presence of the same donor-atom set in isomers **A** and **B**. The broadness of the ^{71}Ga signal is even higher in the ^{71}Ga spectra of $[GaL^{pz*,NH}]^+$ (δ = 53 ppm, $\Delta\nu_{1/2} \sim 12\,000$ Hz) indicating a larger asymmetry of the coordination environment around the trivalent gallium in this complex (Fig. S22†).[26]

In summary, the larger *trans* influence of a phenolate oxygen when compared to an aliphatic amine can certainly account that the pyridyl arm is labile in species **A** but not in species **B**.[27,28] Such *trans* influence may also justify the coordination of both phenoxide groups in the *cis* position relative to the pyrazolyl arm in $[GaL^{pz*,NH}](ClO_4)$, observed either in solution or in the solid state.

Radiolabelling and biological studies

For $H_2L^{pz*,NH}$ and $H_2L^{py,NH}$ that were able to coordinate in an intact form with the Ga^{3+} ion, we have pursued with the study of the synthesis of the respective gallium complexes at a carrier free level using ^{67}Ga. The synthesis of the radiocomplexes was attempted by treating solutions of $^{67}GaCl_3$ in acetate buffer (pH = 5) with ethanolic solutions of the ligands. For a final $H_2L^{py,NH}$ concentration of 6.25×10^{-5} M and after heating at 85 °C for 15 min, the HPLC analysis of the reaction mixture has shown the presence of a single radioactive peak (t_R = 18.3 min). This peak corresponds to $[^{67}GaL^{py,NH}]^+$ since its retention time is well-matched with the one of cold (*i.e.* non-radioactive) $[GaL^{py,NH}]^+$ (t_R = 18.2 min) (Fig. 7a). $[^{67}GaL^{py,NH}]^+$ was obtained in almost quantitative radiochemical yield (RCY) (RCY > 95%), as confirmed by the HPLC analysis and thin layer chromatography (TLC) that discarded the presence of radiochemical impurities corresponding to hydrolyzed forms of gallium. In contrast, $H_2L^{pz*,NH}$ provided only very low amounts (<25%) of the desired radioactive compound

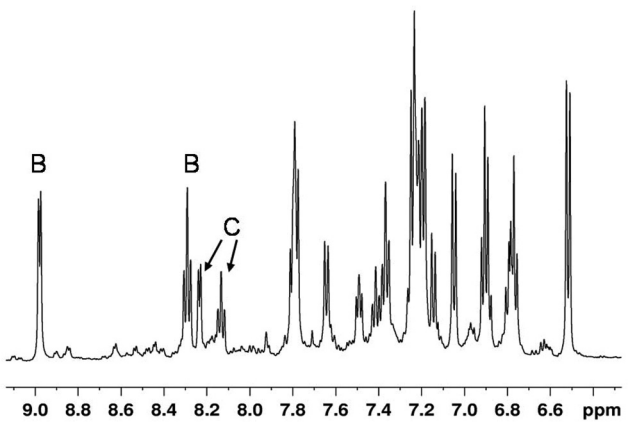

Fig. 6 Aromatic region of the ^{1}H NMR spectra of $[GaL^{py,NH}]^+$ in D_2O showing the presence of two major isomers **B** and **C** in a 1 : 0.7 ratio. Minor peaks are from isomer **A**.

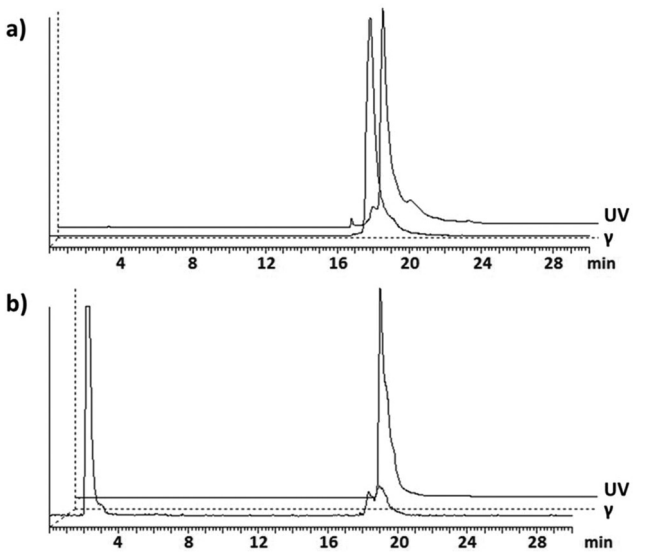

Fig. 7 HPLC chromatograms of: (a) $[GaL^{py,NH}](ClO_4)$ (UV detection) and the reaction mixture of the radiolabeling of $H_2L^{py,NH}$ with $^{67}GaCl_3$ (γ detection); (b) $[GaL^{pz*,NH}](ClO_4)$ (UV detection) and the reaction mixture of the radiolabeling of $H_2L^{pz*,NH}$ with $^{67}GaCl_3$ (γ detection).

($[^{67}\mathbf{GaL}^{\mathbf{pz*,NH}}]^+$) even when a final $\mathbf{H_2L^{pz*,NH}}$ concentration as high as *ca.* 1×10^{-3} M was used (Fig. 7b). These differences are not explained by the weaker basicity of the pyrazolyl arm (pK_a = 2.5 for protonated pyrazole) when compared with the pyridine arm (pK_a = 5.2 for protonated pyridine),[29] as this implies a larger percentage of non-protonated pyrazole available for complexation to the metal.

To have a further insight on the interest of $\mathbf{H_2L^{py,NH}}$ as a new ligand framework for the design of gallium radiopharmaceuticals, we have investigated the *in vitro* stability of $[^{67}\mathbf{GaL}^{\mathbf{py,NH}}]^+$ in challenge experiments with human *apo*-transferrin and we have studied its biodistribution and *in vivo* stability in mice.

The ionic radius of octahedral Ga(III) (0.62 Å) is comparable to that of the high-spin octahedral Fe(III) (0.645 Å). Both these metal ions are hard Lewis acids, which present a strong affinity for hard Lewis bases, in particular to oxygen and nitrogen donors. For these reasons, Ga(III) has a very high affinity for transferrin, which is an iron transport protein with a relatively high concentration (*ca.* 2.5 mg mL^{-1}) in human blood and presenting two homologous regions for iron coordination. Each region can coordinate independently one Fe^{3+} ion (or Ga^{3+}) along with a carbonate or bicarbonate anion per metallic ion. The high affinity of Ga(III) for transferrin explains that radiocomplexes of Ga are usually tested in challenge experiments against this protein, particularly when evaluating new chelator systems,[11,13] as in the present case. These challenge experiments are useful to predict the *in vivo* kinetic inertness of the complexes towards transchelation reactions. $[^{67}\mathbf{GaL}^{\mathbf{py,NH}}]^+$ was incubated with an excess (*ca.* 100 : 1) of *apo*-transferrin in the presence of bicarbonate at 37 °C and the reaction mixture was analysed by HPLC at different time points (Fig. S23†). No transchelation was observed even after 48 h of incubation, which attests for the high *in vitro* stability of $[^{67}\mathbf{GaL}^{\mathbf{py,NH}}]^+$ and for the suitability of $\mathbf{H_2L^{py,NH}}$ to stabilize Ga^{3+} under the conditions involved in the preparation of radiopharmaceuticals. Under the same HPLC analytical conditions, $^{67}GaCl_3$ (t_R = 2.3 min) and **Tf-^{67}Ga** (t_R = 4.3 min) (Fig. S24†) have shown retention times significantly different from that of $[^{67}\mathbf{GaL}^{\mathbf{py,NH}}]^+$, which further validated the results from the challenge experiments.

To ascertain the biokinetics and *in vivo* stability of $[^{67}\mathbf{GaL}^{\mathbf{py,NH}}]^+$, biodistribution studies were carried out in CD-1 mice at 1 h and 4 h after intravenous administration. Total radioactivity excretion was also assessed at both time points. The most relevant data from these studies are summarized in the graphics of Fig. 8. $[^{67}\mathbf{GaL}^{\mathbf{py,NH}}]^+$ shows a fast blood clearance and a moderately fast overall rate of excretion. Noticeably, $[^{67}\mathbf{GaL}^{\mathbf{py,NH}}]^+$ showed a faster blood clearance than ^{67}Ga complexes with pyridyl-containing acyclic chelators of the H_2dedpa type (see Chart 1) which have been recently introduced by Orvig *et al.* According to these authors, the retention of $[\mathbf{^{67}Ga\text{-}dedpa}]^+$ in the blood compartment could be explained by a strong association with serum proteins due to the secondary amine groups of the chelator.[11] Clearly, this is not the case for $[^{67}\mathbf{GaL}^{\mathbf{py,NH}}]^+$ despite the presence of two secondary amines in the structure of the complex.

In general, $[^{67}\mathbf{GaL}^{\mathbf{py,NH}}]^+$ presented a pronounced clearance from most organs and tissues with the exception of those involved in the excretion of the compound, such as the kidney, liver and intestine. In the elimination of the complex, there is a significant contribution of the hepatobiliary excretion pathway despite the moderate hydrophilicity of $[^{67}\mathbf{GaL}^{\mathbf{py,NH}}]^+$ ($\log D_{o/w} = -0.53 \pm 0.04$). The involvement of this excretory route slightly delays the overall radioactivity excretion when compared with Ga-NOTA and with tris(hydroxypyridinone)-based Ga compounds.[13,30,31] Comparably to these Ga chelates, $[^{67}\mathbf{GaL}^{\mathbf{py,NH}}]^+$ also shows a negligible bone uptake (<0.1% I.D. g^{-1} at 4 h p.i.), which indicates a high *in vivo* stability for this complex since it is well known that free Ga^{3+} tends to accumulate in the bone.[32] The *in vivo* stability of $[^{67}\mathbf{GaL}^{\mathbf{py,NH}}]^+$ was further corroborated by radio-HPLC analysis of serum and

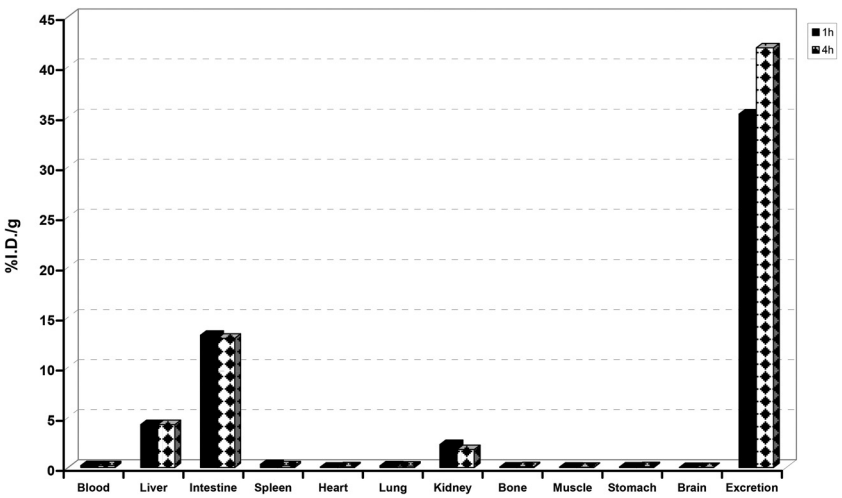

Fig. 8 Biodistribution results of $[^{67}\mathbf{GaL}^{\mathbf{py,NH}}]^+$ in female CD-1 mice showing organ and tissue uptake (expressed in % I.D. g^{-1}) and overall excretion at 1 h and 4 h after i.v. administration.

urine from CD-1 mice injected with this radiocomplex. The obtained radiochromatograms revealed uniquely the presence of intact $[^{67}\mathbf{GaL}^{\mathbf{py,NH}}]^+$ (Fig. S25†). Altogether, the biodistribution profile of $[^{67}\mathbf{GaL}^{\mathbf{py,NH}}]^+$ is consistent with a high *in vivo* stability.

Conclusions

New chelators, $\mathbf{H_2L}^{\mathbf{pz*,NH}}$ and $\mathbf{H_2L}^{\mathbf{py,NH}}$, were designed based on the dien backbone by introducing additional pyrazolyl and pyridyl coordinating units at the central nitrogen atom and by functionalization of the dien terminal amines with phenol groups. The coordination behaviour of these chelators towards the Ga^{3+} ion was evaluated having in mind to assess their suitability for the design of gallium radiopharmaceuticals. For non-radioactive gallium, these studies allowed the synthesis and full characterization by different spectroscopic techniques and X-ray diffraction analysis of $[\mathbf{GaL}^{\mathbf{pz*NH}}]^+$ and $[\mathbf{GaL}^{\mathbf{py,NH}}]^+$ that contain N_4O_2-hexadentate chelators. These complexes have a remarkably different behaviour in solution, as shown by a variety of multinuclear and bidimensional NMR techniques. These studies demonstrated that $[\mathbf{GaL}^{\mathbf{py,NH}}]^+$ exists in solution as a mixture of coordination isomers, while a predominant isomer was detected for $[\mathbf{GaL}^{\mathbf{pz*,NH}}]^+$. At a carrier free level, *i.e.* using radiogallium (^{67}Ga), notorious differences were also observed for the behaviour of $\mathbf{H_2L}^{\mathbf{pz*,NH}}$ and $\mathbf{H_2L}^{\mathbf{py,NH}}$. $[^{67}\mathbf{GaL}^{\mathbf{py,NH}}]^+$ was synthesized in an almost quantitative radiochemical yield using relatively low ligand concentrations (*ca.* 5×10^{-5} M), while $[^{67}\mathbf{GaL}^{\mathbf{2}}]^+$ was hardly formed even using a 50-fold higher concentration of $\mathbf{H_2L}^{\mathbf{pz*,NH}}$. For comparative purposes, the imine congeners $\mathbf{H_2L}^{\mathbf{pz*,C{=}N}}$ and $\mathbf{H_2L}^{\mathbf{py,C{=}N}}$ were also studied but the high reactivity of the imine bonds did not allow the synthesis of Ga(III) complexes with relevance for radiopharmaceutical research.

$[^{67}\mathbf{GaL}^{\mathbf{py,NH}}]^+$ has shown a high *in vivo* stability and a favourable biodistribution profile in mice. Thus, it can be considered as a promising building block for the design of gallium radiopharmaceuticals. It may have relevance for the design of perfusion agents, *e.g.* for cardiac imaging, as different substituents can be introduced at the secondary amines, pyridyl and phenolate rings to tune the lipophilicity of the resulting Ga(III) complexes. However, the $\mathbf{H_2L}^{\mathbf{py,NH}}$ backbone can also be explored to design bifunctional chelators for target-specific radiopharmaceuticals because the pyridyl ring is easily replaceable by picolinic acid derivatives presenting carboxylic groups for linkage to targeting biomolecules.

Altogether, our findings highlighted that the combination of the dien framework with N-heterocyclic and phenol coordinating groups can provide N_4O_2-donor chelators suitable to stabilize Ga(III) complexes for *in vivo* studies. The encouraging results obtained for $\mathbf{H_2L}^{\mathbf{py,NH}}$ justify further studies aiming at a better understanding of the structural factors (*e.g.* nature of the N-heterocyclic group and spacer length) that determine the performance of this type of compounds as chelators for the design of radiopharmaceuticals.

Experimental section

Materials and methods

Unless stated otherwise, the synthesis and work-up of the ligands and complexes were performed under air. The compounds *N*,*N*′-bis(*tert*-butoxycarbonyl)diethylenetriamine (**1**)[33] and (2-{(2-*tert*-butoxycarbonylaminoethyl)-[2-(3,5-dimethylpyrazol-1-yl)-ethyl]amino}ethyl) carbamic acid *tert*-butyl ester (**2**)[23] were prepared according to published methods. $^{67}GaCl_3$ was prepared from the readily available [^{67}Ga]–Gallium Citrate (Mallinckrodt) using SEP-PAK SI cartridges (Waters) as previously reported.[34] The ^{1}H, ^{13}C, ^{71}Ga and ^{15}N NMR spectra of the Ga(III) complexes were recorded at room temperature on a Bruker Avance III spectrometer operating at 500, 125, 152 and 50 MHz, respectively. The ^{1}H and ^{13}C NMR spectra of organic compounds and ligands were recorded on a Varian Unity operating at 300 and 75 MHz, respectively. Chemical shifts of ^{1}H and ^{13}C spectra (δ, ppm) are reported relative to the residual solvent peaks relative to $SiMe_4$. Spectra in D_2O are referenced to TSP. For ^{71}Ga and ^{15}N spectra, external references were used: $Ga(NO_3)_3$ in D_2O (δ = 0 ppm) and neat CH_3NO_2 (δ = 381.7 ppm relative to liquid NH_3), respectively. Peak assignments were achieved *via* the use of COSY, TOCSY, HSQC, NOESY and selective NOEs at 500 MHz. IR spectra were recorded in Nujol using KBr mulls or as KBr pellets on a Bruker, Tensor 27 spectrometer. Electrospray ionisation mass spectrometry (ESI-MS) was performed at Centro de Ciências e Tecnologias Nucleares (C^2TN) on a QITMS instrument in positive ion mode. High resolution-mass spectrometry (HRMS), using ESI-FIA-TOF, was carried out as a service by the University of Santiago de Compostela. For the organic compounds, thin-layer chromatography (TLC) was performed on Merck silica gel 60 F254 plates and column chromatography using silica gel 60 (Merck). RP-TLC of the cold Ga and ^{67}Ga complexes was done using TCL-sheets Alugram RP-18W/UV (Macharey-Nagel) and MeOH/0.9% NaCl (1 : 1) as the eluent. HPLC analysis of the cold Ga and ^{67}Ga complexes was performed on a Perkin-Elmer LC pump 200 coupled to a LC 290 tunable UV-Vis detector and to a Berthold LB-507A radiometric detector, using an analytical Macherey-Nagel C18 reversed-phase column (Nucleosil 100–10, 250 × 4 mm) with a flow rate of 1 mL min^{-1} and gradient elution with a mixture of aqueous 0.9% NaCl (A) and ethanol (B); method: 0–10 min, 100% A; 10–15 min, 100–0% A; 15–25 min, 0% A; 25–26 min, 0–100% A; 26–30 min, 100% A.

Synthesis of *N*′-(2-aminoethyl)-*N*′-[2-(3,5-dimethylpyrazol-1-yl)ethyl]ethane-1,2-diamine (3). To a solution of compound **2** (826 mg, 1.94 mmol) in MeOH (25 mL), at 0 °C, was added 6 mL of 12 M HCl. The reaction mixture was left to stir at room temperature for 24 h. Then, the solvent was evaporated under vacuum, the pH was adjusted to pH = 14 by the addition of 40% aqueous NaOH and the mixture was extracted with dichloromethane (3 × 20 mL). The organic phase was dried over $MgSO_4$, filtered and the filtrate was dried under vacuum to afford the title compound as pale yellow oil. Yield: 341 mg (78%).

HRMS ($C_{11}H_{23}N_5$): *m*/*z* Calcd for $[M + H]^+$, 226.2026; found 226.2018. ^{1}H NMR (293 K, 300 MHz, CD_3OD): δ_H 2.17 (3H, s, CH_3), 2.22 (3H, s, CH_3), 2.51 (4H, tr, CH_2), 2.68 (4H, t, CH_2), 2.82 (2H, t, CH_2), 4.00 (2H, tr, CH_2), 5.75 (1H, s, H(4)-pz). ^{13}C NMR (293 K, 75 MHz, $CDCl_3$): δ_c 10.84 (CH_3), 13.11 (CH_3), 38.96 (CH_2), 38.96 (CH_2), 46.54 (CH_2), 53.68 (CH_2), 55.45 (CH_2), 104.78 (C(4)-pz), 138.58 (C(3/5)-pz), 146.85 (C(3/5)-pz).

Synthesis of *tert*-butyl *N*-[2-[2-(*tert*-butoxycarbonylamino)-ethyl-(2-pyridylmethyl)amino]ethyl]carbamate (4). In a 100 mL flask, **2** (700 mg, 2.26 mmol), 1-bromomethylpyridine (628 mg, 2.48 mmol), K_2CO_3 (685 mg, 4.96 mmol) and KI (41 mg, 0.25 mmol) were mixed in 30 mL dried THF. The mixture was refluxed overnight. The solution was filtered and the solvent was evaporated under reduced pressure to afford the final product. Yield: 786 mg (99%).

HRMS ($C_{20}H_{34}N_4O_4$): *m*/*z* Calcd for $[M + H]^+$, 395.2653; found 395.2650. ^{1}H NMR (293 K, 300 MHz, $CDCl_3$): δ_H 1.42 (18H, s, 2-C$(CH_3)_3$, 2.62 (4H, t, 2-CH_2), 3.15 (4H, t, 2-CH_2), 3.74 (2H, s, CH_2), 5.51 (2H, b, 2-NH), 7.15 (1H, t, py), 7.29 (1H, d, py), 7.62 (1H, t, py), 8.52 (1H, d, py). ^{13}C NMR (293 K, 75 MHz, $CDCl_3$): δ_c 28.32 (CH_3), 38.34 (CH_2), 54.03 (CH_2), 59.80 (CH_2), 78.71 (C$(CH_3)_3$), 121.98 (py), 122.83 (py), 136.37 (py), 148.99 (py), 156.17 (py), 159.37 (C═O).

Synthesis of *N*′-(2-aminoethyl)-*N*′-(2-pyridylmethyl)ethane-1,2-diamine (5). 25 mL of MeOH was added to compound **4** (1.0 g, 2.5 mmol) in a 50 mL flask. The solution was placed in an ice bath and 12 M HCl (6 mL) was added. The mixture was stirred at room temperature for 24 h. The solvent was evaporated under reduced pressure and to the resulting residue was added 40% aqueous NaOH until pH = 14. The compound was then extracted with $CHCl_3$ (3 × 20 mL), dried with $MgSO_4$ and the organic solvent was evaporated under vacuum. Yield: 466 mg (96%).

HRMS ($C_{10}H_{18}N_4$): *m*/*z* Calcd for $[M + H]^+$, 195.1604; found 195.1601. ^{1}H NMR (293 K, 300 MHz, $CDCl_3$): δ_H 2.56 (4H, t, 2-CH_2), 2.73 (4H, t, 2-CH_2), 3.72 (2H, s, CH_2), 7.13 (1H, t, py), 7.37 (1H, d, py), 7.62 (1H, t, py), 8.49 (1H, d, py). ^{13}C NMR (293 K, 75 MHz, $CDCl_3$): δ_c 39.58 (CH_2), 57.59 (CH_2), 60.78 (CH_2), 122.00 (py), 122.89 (py), 136.44 (py), 149.04 (py), 159.83 (py).

Synthesis of $H_2L^{pz*,C=N}$ (2-[(*E*)-2-[2-(3,5-dimethylpyrazol-1-yl)-ethyl-[2-[(*E*)-(2-hydroxyphenyl)methyleneamino]ethyl]amino]-ethyliminomethyl]phenol). A solution of compound **3** (296 mg, 1.31 mmol) and salicylaldehyde (321 mg, 2.63 mmol) in MeOH (15 mL) was refluxed under N_2 for 4 h, and then evaporated to dryness under reduced pressure. The residue was extracted several times with diethyl ether (3 × 25 mL) and the ether fractions were filtered to remove an insoluble orange material. The filtrate was dried under vacuum giving pale yellow oil, which was formulated as $H_2L^{pz*,C=N}$. Yield: 256 mg (45%).

HRMS ($C_{25}H_{31}N_5O_2$): *m*/*z* Calcd for $[M + H]^+$, 434.2551; found 434.2567. IR (KBr, ν/cm^{-1}) 3428w, 3019m, 2952m, 2901m, 2253w, (N═C, sharp) 1634vs, 1582m 1553w, 1498m, 1461m, 1280s, 1216s, 1152w, 1117w, 1072w, 1041w, 900s, 760s, 669sh,m, 650mw, 556w, 464w. ^{1}H NMR (293 K, 300 MHz, $CDCl_3$) δ_H 2.03 (3H, s, CH_3), 2.19 (3H, s, CH_3), 2.83 (4H, t, 2-CH_2), 2.96 (2H, tr, CH_2), 3.54 (4H, tr, 2-CH_2), 3.89 (2H, tr, CH_2), 5.70 (1H, s, H(4)-pz), 6.78 (2H, tr, Ph), 6.90 (2H, d, Ph), 7.00 (2H, d, Ph), 7.26 7.00 (2H, tr, Ph), 8.05 (2H, s, CH═N), 13.38 (2H, br, OH); ^{13}C NMR (293 K, 75 MHz, $CDCl_3$) δ_c 10.84 (CH_3), 13.49 (CH_3), 47.08 (CH_2), 54.93 (CH_2), 55.73 (CH_2), 57.84 (CH_2), 104.77 (C(4)-pz), 116.91 (Ph), 118.46 (Ph), 118.66 (Ph), 131.27 (Ph), 132.11 (Ph), 139.35 (C3/5-pz), 147.32 (C3/5-pz), 161.16 (Ph), 165.95 CH═N).

Synthesis of $H_2L^{pz*,NH}$ (2-[[2-[2-(3,5-dimethylpyrazol-1-yl)-ethyl-[2-[(2-hydroxyphenyl)methylamino]ethyl]amino]ethyl-amino]methyl]phenol). A solution of compound **3** (390 mg, 1.73 mmol) and salicylaldehyde (423 mg, 3.46 mmol) in MeOH (20 mL) was refluxed under N_2 for 4 h. After cooling to room temperature, solid $NaBH_4$ (200 mg, 5.29 mmol) was added to the reaction mixture and the resulting clear solution was stirred overnight at room temperature. The solvent was evaporated under reduced pressure, the oily residue was redissolved in dichloromethane and then washed with a saturated $NaHCO_3$ aqueous solution. The organic phase was separated, the solvent was removed under vacuum and the crude was purified by silica-gel column chromatography using CH_2Cl_2/MeOH/NH_4OH (90/30/2) as the eluent. Removal of the solvent from the collected fractions gave $H_2L^{pz*,NH}$ as transparent oil. Yield: 423 mg (56%).

R_f (SiO_2, $CHCl_3$/MeOH/NH_4OH (90/30/2)) = 0.40. HRMS ($C_{25}H_{35}N_5O_2$): *m*/*z* Calcd for $[M + H]^+$, 438.2864; found 438.2858. IR (KBr, ν/cm^{-1}) 3286w, 3239w, 2951m, 2840m, 2361w, 1591s, 1552m, 1459s, 1419m, 1260s, 1184w, 1151w, 1104m, 1025m, 933w, 845w, 802wm, 756s, 720w, 625w, 544w, 458w. ^{1}H NMR (293 K, 300 MHz, $CDCl_3$) δ_H 1.87 (3H, s, CH_3), 2.20 (3H, s, CH_3), 2.56 (4H, m, 2-CH_2), 2.62 (2H, m, CH_2), 2.74 (2H, tr, CH_2), 3.89 (4H, s, CH_2), 4.01 (2H, tr, CH_2), 5.71 (1H, s, H(4)-pz), 6.75–6.81 (4H, tr, Ph), 6.98 (2H, d, Ph), 7.13 (2H, d, Ph); ^{13}C NMR (293 K, 75 MHz, $CDCl_3$) δ_c 10.70 (CH_3), 12.69 (CH_3), 45.62 (CH_2), 46.56 (CH_2), 52.06 (CH_2), 53.28 (CH_2), 53.54 (CH_2), 105.04 (C(4)-pz), 115.96 (Ph), 118.60 (Ph), 122.21 (Ph), 128.25 (Ph), 128.27 (Ph), 134.41 (C3/5-pz), 146.98 (C3/5-pz), 158.06 (Ph).

Synthesis of $H_2L^{py,C=N}$ (2-[(*E*)-2-[2-[(*E*)-(2-hydroxyphenyl)-methyleneamino]ethyl-(2-pyridylmethyl)amino]ethyliminomethyl]phenol). Compound **5** (440 mg, 2.26 mmol) and salicylaldehyde (552 mg, 476 μL, 4.52 mmol) were dissolved in dried MeOH (10 mL). The mixture was refluxed under N_2 for 3 h. After evaporation of the solvent, the crude product was extracted with diethyl ether. The ether was dried under reduced pressure to afford the final product in the form of yellow oil. Yield: 774 mg (85%).

HRMS ($C_{24}H_{26}N_4O_2$): *m*/*z* Calcd for $[M + H]^+$, 403.2129; found 403.2132. IR (KBr, ν/cm^{-1}) 3059w, 3009w, 2846w, 2362w, 1634s, 1588m, 1498m, 1460m, 1372w, 1280m, 1208w, 1152m, 1116m, 1077m, 895w, 85w, 757s, 641w, 624w, 558w, 460w. ^{1}H NMR (293 K, 300 MHz, $CDCl_3$) δ_H 2.89 (4H, t, 2-CH_2), 3.62 (4H, t, 2-CH_2), 3.82 (2H, s, CH_2), 6.76 (4H, t, Ph), 6.91 (2H, d, Ph), 6.97 (2H, d, Ph), 711 (1H, t, py), 7.27 (1H, d, py), 7.41 (1H, t, py), 8.05 (2H, s, 2-N═CH), 8.51 (1H, d, py). ^{13}C NMR (293 K,

75 MHz, $CDCl_3$): δ_c 55.28 (CH_2), 57.50 (CH_2), 60.84 (CH_2), 116.83 (Ph), 118.35 (Ph), 118.60 (Ph), 121.94 (py), 122.78 (py), 131.18 (Ph), 132.00 (Ph), 136.42 (py), 148.72 (py), 159.42 (py), 161.10 (Ph), 165.76 (N=CH).

Synthesis of $H_2L^{py,NH}$ (2-[[2-[2-[(2-hydroxyphenyl)methylamino]ethyl-(2-pyridylmethyl)amino]ethylamino]methyl]phenol). To a solution of $H_2L^{py,C=N}$ (362 mg, 0.9 mmol) in MeOH (10 mL), $NaBH_4$ (102 mg, 2.7 mmol) was added. The solution was stirred overnight at room temperature. The solvent was evaporated under reduced pressure, the oily residue was redissolved in dichloromethane and filtered. The solvent was removed under vacuum and the residue was washed with diethyl ether. After drying under vacuum, the final compound was obtained as dark brown oil. Yield: 353 mg (97%).

HRMS ($C_{24}H_{30}N_4O_2$): *m*/*z* Calcd for $[M + H]^+$, 407.2442; found 407.2447. IR (KBr, ν/cm^{-1}) 3418s (N–H), 3418s, 3054m, 2948m, 2845m, 2362w, 1592vs, 1475 s, 1435sh,s, 1260s, 1151m, 1104m, 1000w, 936w, 843w, 756s, 736m, 702w, 624w, 459w. ^{1}H NMR (293 K, 300 MHz, $CDCl_3$) δ_H 2.64 (8H, m, 4-CH_2), 3.66 (2H, s, CH_2), 3.80 (4H, s, 2-CH_2), 5.23 (s, NH), 6.71 (4H, t, Ph), 6.85 (2H, d, Ph), 7.05–7.20 (4H, m, Ph + py), 7.59 (1H, t, py), 8.40 (1H, d, py). ^{13}C NMR (293 K, 75 MHz, $CDCl_3$): δ_c 45.93 (CH_2), 52.44 (CH_2), 54.22 (CH_2), tah60.19 (CH_2), 116.21 (Ph), 118.82 (Ph), 122.53 (py), 122.80 (py), 123.32 (Ph), 128.25 (Ph), 128.48 (Ph), 136.63 (py), 149.37 (py), 158.16 (Ph), 159.10 (py).

Synthesis of $[GaL^{pz*,NH}](ClO_4)$. To a solution of $Ga(NO_3)_3{\cdot}10H_2O$ (100 mg, 0.23 mmol) in MeOH (5 mL) was added dropwise a solution of $H_2L^{pz*,NH}$ (125 mg, 0.29 mmol) also in MeOH (2 mL). To the resulting clear solution was added $NaCH_3COO{\cdot}3H_2O$ (80 mg, 0.59 mmol) dissolved in 5 mL of MeOH, and the reaction mixture was stirred overnight at room temperature. The mixture was treated with $NaClO_4{\cdot}H_2O$ (40 mg, 0.29 mmol) and let to stand overnight in the refrigerator. The formed white precipitate was separated by filtration, dried and formulated as $[GaL^{pz*,NH}](ClO_4)$. Yield: 52 mg (34%).

Anal. Calcd for $C_{25}H_{33}ClGaN_5O_6{\cdot}3CH_3OH$ (668.82): C, 47.98; H, 6.47; N, 9.99; found: C, 47.50; H, 6.85; N, 10.10. ESI-MS: *m*/*z* calcd for $[M]^+$, 504.2; found: 504.2. IR (KBr, ν/cm^{-1}) 3429m (N–H), 3238w, 2926w, 1548m, 1483s, 1454m, 1298m, 1274m, 1085s, 881mw, 756mw, 622mw, 524w, 476w. t_R = 17.5 min. R_f = 0.2. ^{1}H NMR (293 K, 500 MHz $CDCl_3$) δ_H 2.35 (6H, s, CH_3), 2.20 (H, m, CH_2), 2.50 (1H, dd, CH_2), 2.63 (1H, dd, CH_2), 2.73 (1H, m, CH_2), 2.90 (1H, m, CH_2), 3.20–3.00 (4H, m, CH_2), 3.69–3.49 (4H, m, 2NH + 2CH_2), 3.74 (1H, d, CH_2), 3.97 (1H, t, CH_2), 4.22 (1H, t, CH_2), 4.45 (1H, d, CH_2), 4.74 (1H, d, CH_2), 6.14 (1H, s, H(4)-pz), 6.40 (1H, d, Ph), 6.59 (1H, t, Ph), 6.66 (1H, t, Ph), 6.78 (1H, d, Ph), 7.04 (1H, d, Ph), 7.11 (1, t, Ph), 7.18 (1H, t, Ph); ^{13}C NMR (293 K, 125 MHz, CD_3CN) δ_C 11.27 (CH_3), 14.15 (CH_3), 41.395 (CH_2), 44.02 (CH_2), 45.44 (CH_2), 50.69 (CH_2), 51.71 (CH_2), 52.78 (CH_2), 56.83 (CH_2), 108.66 (C(4)-pz), 116.312 (Ph), 116.77 (Ph), 118.99 (Ph), 120.96 (Ph), 121.70 (Ph), 123.12 (Ph), 129.74 (Ph), 130.13 (Ph), 130.81 (Ph), 145.03 (C(5)-pz), 153.03 (C(3)-pz), 161.37 (Ph), 164.06 (Ph); ^{71}Ga NMR (293 K, 152 MHz, CD_3CN) δ_{Ga} 53; ^{15}N NMR (293 K, 51 MHz, CD_3CN): δ_N 30.2 (NH *trans* to pyrazolyl), 42.0 (NH in equatorial position).

Synthesis of $[GaL^{py,NH}](ClO_4)$. To a solution of $H_2L^{py,NH}$ (173 mg, 0.43 mmol) in MeOH (10 mL) was added a $Ga(NO_3)_3{\cdot}10H_2O$ (148 mg, 0.34 mmol) also in MeOH (5 mL). To the resulting clear solution was added $NaCH_3COO{\cdot}3H_2O$ (70.5 mg, 0.86 mmol) dissolved in 5 mL of MeOH. The reaction mixture was stirred overnight at room temperature. The solution was treated with $NaClO_4{\cdot}H_2O$ (59 mg, 0.43 mmol) and again stirred overnight at room temperature. After removal of the solvent at reduced pressure, the residue was extracted with 5 × 10 mL $CHCl_3$. Evaporation of $CHCl_3$ gave a light brown solid that was recrystallized from methanol to afford $[GaL^{py,NH}](ClO_4)$. Yield: 36 mg (22%).

Anal. Calcd for $C_{24}H_{28}ClGaN_4O_6{\cdot}CH_3OH$ (605.73): C, 49.57; H, 5.32; N, 9.25; found: C, 49.39; H, 5.49; N, 9.18. ESI-MS: *m*/*z* calcd for $[M]^+$ 473.1; found 473.3. IR (KBr, ν/cm^{-1}) 3429m (N–H), 3238w, 2926w, 1548m, 1483s, 1454m, 1298m, 1274m, 1085s, 881mw, 756mw, 622mw, 524w, 476w. t_R = 18.2 min. R_f = 0.2. ^{1}H NMR (293 K, 500 MHz, $CDCl_3$) δ_H 2.52 (1H, m, CH_2), 2.67 (1H, d–d, CH_2), 2.88 (1H, d–d, CH_2), 3.03 (2H, m, CH_2), 3.26 (2H, m, CH_2), 3.63 (4H, m, 2-CH_2), 4.03 (1H, d, CH_2), 4.32 (1H, d, NH), 4.34 (2H, m, CH_2), 4.72 (1H, d, NH), 6.38 (1H, d, Ph), 6.56 (1H, t, Ph), 6.72 (1H, t, Ph), 6.96 (2H, t, ph), 7.06 (2H, d, Ph), 7.21 (1H, d, Ph), 7.61 (2H, m, py), 8.1 (1H, t, py), 9.05 (1H, d, py); ^{13}C NMR (293 K, 125 MHz, CD_3CN) δ_C 42.37 (CH_2), 42.78 (CH_2), 44.31 (CH_2), 44.93 (CH_2), 51.71 (CH_2), 52.14 (CH_2), 52.71 (CH_2), 54.09 (CH_2), 54.62 (CH_2), 55.66 (CH_2), 56.50 (CH_2), 57.84 (CH_2), 58.32 (CH_2), 63.00 (CH_2), 78.65 (CH_2), 116.23 (Ph), 119.37 (Ph), 121.14 + 121.50 (py), 123.64 + 124.57 + 125.56 (Ph), 129.96 + 130.54 + 131.13 (Ph), 142.14 + 142.57 (py), 146.73 (py), 148.55 (py), 153.93 (py), 163.48 + 164.28 (Ph); ^{71}Ga NMR (293 K, 152 MHz, CD_3CN) δ_{Ga} 102; ^{15}N NMR (293 K, 51 MHz, CD_3CN) δ_N 26.7 (NH_a(A) + NH_b(B)), 38.5 (NH_b(A)), 41.3 (NH_b(B)).

X-ray crystallography

Crystals suitable for X-ray diffraction analysis were mounted on a loop with protective oil. The X-ray diffraction data for compounds $[GaL^{pz*,NH}](ClO_4)$ (MeOH), $[GaL^{pz*,NH}](ClO_4){\cdot}(CHCl_3)$, $[GaL^{py,NH}](ClO_4){\cdot}$(MeOH) and $[GaL^{pz*,OMe}](ClO_4){\cdot}$(MeOH) (see ESI†) were collected on a Bruker APEXII CCD diffractometer using graphite monochromated Mo-Kα radiation (λ = 0.71069 Å), equipped with an Oxford Cryosystems low-temperature device at 150 K, operated in the ω and φ scans mode. A semi-empirical absorption correction was carried out using SADABS.[35] Data collection, cell refinement and data reduction were done with the SMART and SAINT programs.[36] The structures were solved by direct methods using SIR97[37] and refined by full-matrix least-squares methods with the SHELXL97[38] program using the WINGX[39] software package. A full-matrix least-squares refinement was used for the non-hydrogen atoms with anisotropic thermal parameters. All hydrogen atoms connected to carbons were inserted in idealized positions and allowed to refine riding in the parent

carbon atom; hydrogen atoms bonded to nitrogen atoms were located in a difference map. Molecular graphics were prepared using MERCURY 1.4.2.[40]

CCDC-964822 (for $[GaL^{pz*,OMe}](ClO_4)\cdot(MeOH)$), -964823 (for $[GaL^{pz*,NH}](ClO_4)\cdot(CHCl_3)$), -964824 (for $[GaL^{pz*,NH}](ClO_4)\cdot(MeOH)$) and 964825 (for $[GaL^{py,NH}](ClO_4)$ (MeOH)) contain the supplementary crystallographic data for this paper.

Labeling of $H_2L^{pz*,NH}$ and $H_2L^{puy,NH}$ with ^{67}Ga. To 80 μL of $H_2L^{pz*,NH}$ in EtOH (5×10^{-3} M) or to 20 μL of $H_2L^{py,NH}$ in EtOH (1×10^{-3} M) was added 200 μL of acetate buffer (0.4 M, pH ≈ 5) and then 100 μL of $^{67}GaCl_3$ (0.1 M HCl). The reaction mixtures were heated at 85 °C for 15 min and, after cooling to room temperature, were analysed by radio-HPLC and RP-TLC. HPLC analysis showed that $[^{67}GaL^{pz*,NH}]^+$ was formed in very low RCY (<25%) while $[^{67}GaL^{py,NH}]^+$ was obtained almost quantitatively (RCY > 95%).

The *in vitro* stability of $[^{67}GaL^{py,NH}]^+$ was studied in challenge experiments against human *apo*-transferrin. In these challenge experiments, 300 μL of $[^{67}GaL^{py,NH}]^+$ solution were added to 1.2 mL of *apo*-transferrin (3 mg mL^{-1}) solution in $NaHCO_3$ (10 mM). The mixture was maintained at 37 °C for 2 days and analysed by HPLC at 0 h, 1 h, 24 h and 48 h. The lipophilicity of $[^{67}GaL^{py,NH}]^+$ was assessed by the measurement of the log $D_{o/w}$ value under physiological conditions (*n*-octanol/0.1 M PBS, pH = 7.4) using the "shake-flask" method.[41]

$$[^{67}GaL^{py,NH}]^+ : R_f = 0.2;\ t_R = 18.3 \text{ min};$$
$$\log D_{o/w} = -0.53 \pm 0.04.$$

Biodistribution and *in vivo* stability studies

Animal experiments were conducted in conformity with the national law and with the EU Guidelines for Animal Care and Ethics in Animal Experimentation. The animals were housed in a temperature- and humidity-controlled room with a 12 h light/12 h dark schedule.

The biodistribution of the ^{67}Ga-complex was studied in groups of 3 female CD-1 mice (randomly bred, Charles River) weighing approximately 30–35 g each. Animals were intravenously injected with 100 μL (2–3 MBq) of each preparation *via* the tail vein and were maintained on normal diet *ad libitum*. At 1 h and 4 h after administration, each mice group was sacrificed by cervical dislocation. The radioactive dosage administered and the radioactivity in the sacrificed animal was measured in a dose calibrator (Capintec CRC25R). The difference between the radioactivity in the injected and sacrificed animal was assumed to be due to excretion, mainly urinary excretion. Blood samples were taken by cardiac puncture at sacrifice. Tissue samples of the main organs were then removed, weighed and counted in a gamma counter (Berthold, LB2111, Germany). Accumulation of radioactivity in the tissues was calculated and expressed as percentage of the injected radioactivity per gram of organ (% I.D. g^{-1}) or in percentage of the injected radioactivity per organ (% I.D. per organ) (Tables S3 and S4†). For blood, bone and muscle, total activity was calculated assuming that these organs constitute 6, 10 and 40% of the total weight, respectively. Urine was also collected at sacrifice time.

The *in vivo* stability of the complexes was assessed by urine and murine serum analysis by HPLC under the experimental conditions described for radiochemical purity evaluation.

Urine. Urine was collected at sacrifice time, it was centrifuged and then aliquots were analysed by RP-HPLC.

Serum. Blood collected from mice was centrifuged immediately for 15 min at 3000 rpm at 4 °C and the serum separated. Afterwards aliquots of 100 μL of serum were treated with 200 μL of ethanol to precipitate the proteins. Samples were cooled at 4 °C and centrifuged at 4000 rpm for 15 min. Supernatant was collected and passed through a Millex GV filter (0.22 μm) prior to RP-HPLC analysis.

Acknowledgements

Fundação para a Ciência e Tecnologia (FCT) is acknowledged for financial support (EXCL/QEQ-MED/0233/2012 and RECI/QEQ-QIN/0189/2012). F. Silva thanks FCT for the doctoral research grant (SFRH/BD/47308/2008). COST Action TD1004 is also acknowledged. J. Marçalo is acknowledged for the ESI-MS analyses which were run on a QITMS instrument acquired with the support of the Programa Nacional de Reequipamento Científico (Contract REDE/1503/REM/2005 – ITN) of FCT and is part of RNEM – Rede Nacional de Espectrometria de Massa.

References

1 T. J. Wadas, E. H. Wong, G. R. Weisman and C. J. Anderson, *Chem. Rev.*, 2010, **110**, 2858–2902.
2 M. D. Bartholomä, A. S. Louie, J. F. Valliant and J. Zubieta, *Chem. Rev.*, 2010, **110**, 2903–2920.
3 B. M. Zeglis and J. S. Lewis, *Dalton Trans.*, 2011, **40**, 6168–6195.
4 J. D. G. Correia, A. Paulo, P. D. Raposinho and I. Santos, *Dalton Trans.*, 2011, **40**, 6144–6167.
5 E. W. Price and C. Orvig, *Chem. Soc. Rev.*, 2014, **43**, 260–290.
6 C. E. Ramogida and C. Orvig, *Chem. Commun.*, 2013, **49**, 4720–4739.
7 F. Rosch, *Appl. Radiat. Isot.*, 2013, **76**, 24–30.
8 G. R. Morais, A. Paulo and I. Santos, *Organometallics*, 2012, **31**, 5693–5714.
9 P. Antunes, M. Ginj, H. Zhang, B. Waser, R. P. Baum, J. C. Reubi and H. Maecke, *Eur. J. Nucl. Med. Mol. Imaging*, 2007, **34**, 982–993.
10 M. Eder, B. Wängler, S. Knackmuss, F. LeGall, M. Little, U. Haberkorn, W. Mier and M. Eisenhut, *Eur. J. Nucl. Med. Mol. Imaging*, 2008, **35**, 1878–1888.
11 E. Boros, C. L. Ferreira, J. F. Cawthray, E. W. Price, D. W. Wester, M. J. Adam and C. Orvig, *J. Am. Chem. Soc.*, 2010, **132**(44), 15726–15733.

12 G. A. Bailey, E. W. Price, B. M. Zeglis, C. L. Ferreira, E. Boros, M. J. Lacasse, B. O. Patrick, J. S. Lewis, M. J. Adam and C. Orvig, *Inorg. Chem.*, 2012, **51**(22), 12575–12589.

13 D. J. Berry, Y. Ma, J. R. Ballinger, R. Tavaré, A. Koers, K. Sunassee, T. Zhou, S. Nawaz, G. E. D. Mullen, R. C. Hider and P. J. Blower, *Chem. Commun.*, 2011, **47**, 7068–7070.

14 C. S. Cutler, M. C. Giron, D. E. Reichert, A. Z. Snyder, P. Herrero, C. J. Anderson, D. A. Quarless, S. A. Koch and M. J. Welch, *Nucl. Med. Biol.*, 1999, **26**, 305–316.

15 Y.-M. Hsiao, C. J. Mathias, S.-P. Wey, P. E. Fanwick and M. A. Green, *Nucl. Med. Biol.*, 2009, **36**(1), 39–45.

16 T. Oliver, D. Wolfgang, M. Felner, H.-G. Buchholz, N. Bausbacher, M. Schreckenberger and F. Rösch, *Eur. J. Nucl. Med. Mol. Imaging*, 2010, **37**, 1935–1942.

17 F. Mendes, A. Paulo and I. Santos, *Dalton Trans.*, 2011, **40**, 5377–5393.

18 F. Silva, F. Marques, I. C. Santos, A. Paulo, A. S. Rodrigues, J. Rueff and I. Santos, *J. Inorg. Biochem.*, 2010, **104**, 523–532.

19 R. Garcia, P. Fouskova, L. Gano, A. Paulo, P. Campello, E. Toth and I. Santos, *J. Biol. Inorg. Chem.*, 2009, **14**, 261–271.

20 S. R. Banerjee, M. Pullambhatla, C. A. Foss, A. Falk, Y. Byun, S. Nimmagadda, R. C. Mease and M. G. Pomper, *J. Med. Chem.*, 2013, **56**(15), 6108–6121.

21 L. Maria, C. Fernandes, R. Garcia, L. Gano, A. Paulo, I. C. Santos and I. Santos, *Dalton Trans.*, 2009, 603–606.

22 L. R. Goethals, I. Santos, V. Caveliers, A. Paulo, F. De Geeterb, L. Gano, C. Fernandes and T. Lahoutte, *Contrast Media Mol. Imaging*, 2011, **6**, 178–188.

23 E. Pérez-Mayoral, E. Soriano, S. Cerdán and P. Ballesteros, *Molecules*, 2006, **11**, 345–356.

24 S. E. Harpstrite, A. A. Beatty, S. D. Collins, A. Oksman, D. E. Goldberg and V. Sharma, *Inorg. Chem.*, 2003, **42**(7), 2294–2300.

25 R. Shakya, F. Peng, J. Liu, M. J. Heeg and C. N. Verani, *Inorg. Chem.*, 2006, **45**, 6263–6268.

26 D. Parker, B. P. Waldron and D. S. Yufit, *Dalton Trans.*, 2013, **42**, 8001–8008.

27 G. Berana, A. J. Carty, H. A. Patelan and G. J. Palenik, *Chem. Commun.*, 1970, 222–223.

28 I. Sinclair, R. W. H. Small and I. J. Worrall, *Acta Crystallogr., Sect. B: Struct. Crystallogr. Cryst. Chem.*, 1981, **B37**, 1290–1292.

29 R. Marion, N. M. Saleh, N. Le Poul, D. Floner, O. Lavastrec and F. Geneste, *New J. Chem.*, 2012, **36**, 1828–1835.

30 M. I. M. Prata, A. C. Santos, C. F. G. C. Geraldes and J. J. P. Lima, *Nucl. Med. Biol.*, 1999, **26**, 707–710.

31 S. Chaves, S. M. Marques, A. M. F. Matos, A. Nunes, L. Gano, T. Tuccinardi, A. Martinelli and M. A. Santos, *Chem. – Eur. J.*, 2010, **16**, 10535.

32 R. G. Sephton, G. S. Hodgson, S. D. Abrew and A. W. Harris, *J. Nucl. Med.*, 1978, **19**, 930–935.

33 S. R. Lane, B. Veerendra, T. L. Rold, G. L. Sieckman, T. J. Hoffman, S. S. Jurisson and C. J. Smith, *Nucl. Med. Biol.*, 2008, **35**(3), 263–272.

34 V. Scasnár and J. E. V. Lier, *Eur. J. Nucl. Med.*, 1993, **20**, 273.

35 G. M. Sheldrick, *SADABS*, Bruker AXS Inc., Madison, Wisconsin, USA, 2004.

36 *Bruker, SMART and SAINT*, Bruker AXS Inc., Madison, Wisconsin, USA, 2004.

37 A. Altomare, M. C. Burla, M. Camalli, G. L. Cascarano, C. Giacovazzo, A. Guagliardi, A. G. G. Moliterni, G. Polidori and R. Spagna, *J. Appl. Crystallogr.*, 1999, **32**, 115–119.

38 G. M. Sheldrick, *SHELXL97, Program for Crystal Structure Refinement*, University of Goettingen, Germany, 1997.

39 L. J. Farrugia, *J. Appl. Crystallogr.*, 1999, **32**, 837–838.

40 C. F. Macrae, P. R. Edgington, P. McCabe, E. Pidcock, G. P. Shields, R. Taylor, M. Towler and J. Van de Streek, *J. Appl. Crystallogr.*, 2006, **39**, 453–457.

41 D. E. Troutner, W. A. Volkert, T. J. Hoffman and R. A. Holmes, *Int. J. Appl. Radiat. Isot.*, 1984, **35**, 467–470.